

Drift vs Shift: Decoupling Trends and Changepoint Analysis

Haoxuan Wu, Sean Ryan and David S. Matteson *

Department of Statistics and Data Science, Cornell University

hw399@cornell.edu, matteson@cornell.edu

Abstract

We introduce a new approach for decoupling trends (drift) and changepoints (shifts) in time series. Our locally adaptive model-based approach for robustly decoupling combines Bayesian trend filtering and machine learning based regularization. An over-parameterized Bayesian dynamic linear model (DLM) is first applied to characterize drift. Then a weighted penalized likelihood estimator is paired with the estimated DLM posterior distribution to identify shifts. We show how Bayesian DLMs specified with so-called shrinkage priors can provide smooth estimates of underlying trends in the presence of complex noise components. However, their inability to shrink exactly to zero inhibits direct changepoint detection. In contrast, penalized likelihood methods are highly effective in locating changepoints. However, they require data with simple patterns in both signal and noise. The proposed decoupling approach combines the strengths of both, i.e. the flexibility of Bayesian DLMs with the hard thresholding property of penalized likelihood estimators, to provide changepoint analysis in complex, modern settings. The proposed framework is outlier robust and can identify a variety of changes, including in mean and slope. It is also easily extended for analysis of parameter shifts in time-varying parameter models like dynamic regressions. We illustrate the flexibility and contrast the performance and robustness of our approach with several alternative methods across a wide range of simulations and application examples.

Keywords: Structural Change; Stochastic Volatility; Dynamic Linear Models; Trend Filtering; Posterior Summary

*The authors gratefully acknowledge financial support from the National Science Foundation 1455172, 1934985, 1940124, 1940276, 2114143, and USAID 7200AA18CA00014.

1 Introduction

Distinguishing between global or macro patterns and local or micro fluctuations helps summarize the evolution of complex non-stationary dynamic systems. Herein, we focus on making distinctions between drift and shifts. Drift describes the micro-level evolution of a process. This may appear as variation about gradual trends. In contrast, shifts refer to discontinuities, rapid changes, or major breaks in trend. These represent macro-level changes in a process. Both trends and shifts might be mechanistically or stochastically generated and/or modeled. However, the underlying causes of shifts are typically different from those of drift. While understanding such differences is a prime scientific objective, this first requires distinguishing drift from shifts.

A commonly used approach for modeling drift in time series regression is the dynamic linear model (DLM). Herein, we focus on Bayesian estimation of DLMs, but more broadly, DLMs are hierarchical models in which observed variables are modeled as function of latent variables or parameters that dynamically evolve over time (Chan and Eisenstat, 2018). Although the DLM is specified by a linear relationship at any fixed time, in allowing latent process level parameters to change over time, the DLM provides great flexibility and wide applicability for modeling complex dynamics in time series data. For examples, Bayesian DLMs have important applications in economics (Nakajima *et al.*, 2011), climate analysis (Pichuka and Maity, 2018) and financial markets (Guidolin *et al.*, 2019).

To ensure sufficient flexibility, Bayesian DLMs tend to be heavily overparameterised models (with at least one parameter per data point). As a result, they are typically applied alongside shrinkage priors which produce smoother and more reliable estimates for the dynamic features by “shrinking” small changes closer to zero. Various forms of shrinkage priors such as the horseshoe prior (Carvalho *et al.*, 2009), double-gamma prior (Bitto and Fruhwirth-Schnatter, 2019), double exponential prior (Park and Casella, 2008) and dynamic horseshoe (Kowal *et al.*, 2019) have shown to be effective. When used in conjunction with shrinkage priors, DLMs are excellent for capturing changes that occur smoothly over time. However, since the priors do not shrink parameters exactly to zero, they often struggle to capture sudden breaks, such as changepoints.

Within the changepoint literature, many different approaches have been taken for identifying sudden breaks (Aminikhanghahi and Cook, 2017). Likelihood ratio tests using various forms of cumulative statistics have been utilized to select an optimal partitioning (Jeske *et al.*, 2009; Fryzlewicz, 2014). However, these methods typically rely on the data fitting a pre-specified parametric

model and lack flexibility to adapt to more complex datasets. Penalized likelihood approaches have been utilized to optimize a cost function balancing trade-off between goodness-of-fit and number of changepoints (Killick *et al.*, 2012; Bai and Perron, 2002; Maidstone *et al.*, 2017). Other approaches such as non-parametric distanced based metrics (Matteson and James, 2014; James and Matteson, 2014; Harchaoui *et al.*, 2008), Bayesian probabilistic modeling (Erdman and Emerson, 2008; Zhang *et al.*, 2019; Adams and MacKay, 2007) and subspace identification (Liu *et al.*, 2013) have also been utilized to identify changepoints. While these methods have shown to be effective on well-behaved time series, they tend to struggle when we combine stationary and non-stationary models.

Due to the discrete nature of the changepoint problem, estimating changepoints in a Bayesian setting is very challenging. A number of authors developed changepoint models for which it is possible to generate iid samples from the posterior (Fearnhead, 2006; Fearnhead and Liu, 2011); however, these methods require relatively simple changepoint models and struggle to take account of stochastic volatility or heavy tailed errors. More complex models can be estimated via Markov chain based sampling such as reversible jump MCMC (Green, 1995) and Metropolis Hastings (Green, 2003); however, these methods are known to struggle to converge in practice (Eckley *et al.*, 2011). More recently, Ko *et al.* (2015) investigates the use of hidden markov models with Dirichlet priors for changepoint analysis; however, the authors only consider settings with one or two unambiguous changepoints. Furthermore, even in settings where the posterior can be easily sampled, it can be challenging to interpret the resulting uncertainty estimates since the uncertainty applies to both the changepoint estimates and the number of changepoints (Siems *et al.*, 2019). Thus, inference is typically partitioned conditional on the number of changepoints.

Given the complementary strengths of Bayesian DLMS and changepoint models, it is natural to ask whether these methods can be combined in some way. In this paper, we propose a Bayesian method called the decoupled approach that allows us to identify changepoints in any Bayesian dynamic linear model. The decoupled approach consists of two steps. First, a Bayesian dynamic linear model will be utilized to separate the true signal of the data from the noise components. We do not specify a particular structure for the dynamic linear model but rather will show the approach works for a wide range of structures. Second, a regularized loss will be imposed on the posterior of the model to estimate changepoints.

The decoupled approach extends ideas developed by Hahn and Carvalho (2015) which separates the processes of regression modeling and inference. In their work, the authors focused on the problem of variable selection in linear regression. For the modeling step, a Bayesian linear regression

model is fit to estimate the coefficients associated with a set of predictors. For the inference step, a penalized loss function is placed on posterior mean of the coefficient estimates to select a sparse set of predictors that can be predictive of the response variable. In essence, the paper introduces a two-step Bayesian framework for sparse model summaries. Since then, this approach has been shown to be effective in a variety of other contexts such as sparse graph estimation (Bashir *et al.*, 2019), portfolio optimization (Puelz *et al.*, 2015) and Bayesian function-on-scalar regression (Kowal and Bourgeois, 2020). In this paper, we extend the decoupled approach to non-stationary time series analysis.

The decoupled approach provides two key advantages. First, the decoupled approach separates the process of Bayesian trend modeling from changepoint estimation. As we will illustrate in Section 2, only the trend component of the Bayesian model will be used to identify changepoints. As a result, we can fit a highly flexible Bayesian model to deal with the intricacies of the data such as outliers, heterogeneity and seasonality. Most existing changepoint algorithms struggle to deal with these components as they tend to significantly skew the distribution of the data and violate distributional assumption. By separating the processes of trend-filtering and changepoint estimation, we can create a highly robust framework that can deal with all these issues. Second, by using a regularized loss on the posterior of the Bayesian model, the decoupled approach is able to provide uncertainty estimates for the number of changepoints selected. The loss is marginalized over all values of the penalty parameter and MCMC draws from the posterior can be used to estimate uncertainty. In turn, the decoupled approach can provide more insights into the selection process and the trade-off between goodness-of-fit and the number of changepoints.

This paper proceeds as follows. In Section 2, we introduce the decoupled approach for identifying changepoints in Bayesian dynamic linear models, define diagnostic tools for selection of optimal number of changepoints and detail extensions to covariates/multiple predictors. We also discuss the benefits of using shrinkage priors in Bayesian DLMS. Section 3 illustrates the effectiveness of the decoupled approach in diverse sets of simulation scenarios. We compare the decoupled approach with a variety of other changepoint methods for both change in mean and change in regression coefficients. The robustness of the decoupled approach will be shown through examples with outliers and heteroskedasticity. Section 4 further illustrates the effectiveness of the decoupled approach through two real-world datasets. We conclude with a discussion of the overall framework and its key benefits.

2 Methodology

2.1 Decoupled Modeling

To introduce the decoupled approach, we start by utilizing a standard Bayesian dynamic linear models. Suppose we are given a time series $\mathbf{Y} = (y_1, \dots, y_n)'$ and a predictor series $\mathbf{X} = (x_1, \dots, x_n)'$, a Bayesian DLM can be formulated as follows:

$$\begin{aligned} y_t &= x_t \beta_t + \epsilon_t, & \epsilon_t &\sim N(0, \sigma_{\epsilon,t}^2) \\ \Delta^D \beta_t &= \omega_t & \omega_t &\sim N(0, \sigma_{\omega}^2) \end{aligned} \tag{1}$$

In this setup, $\{\beta_t\}$ models with the time-varying relationship between the predictor series $\{x_t\}$ and the response series $\{y_t\}$. As an example, to estimate changes in mean for $\{y_t\}$, we can set $x_t = 1$ for $t = 1, \dots, n$. The process $\{\epsilon_t\}$ models noise; $\{\sigma_{\epsilon,t}^2\}$ is modeled as potentially time varying; a heteroskedastic noise process gives additional flexibility with low computational cost, in practice. For now, we will assume only one predictor series. Later on, we will extend the framework to deal with multiple predictors.

The primary goal of the Bayesian DLM in this step is to get a preliminary estimate the process $\{\beta_t\}$ and to understand the time-varying relationship between the predictor and the response. We assume the process $\{\beta_t\}$ is a relatively smooth process with occasional large jumps, which will be regarded as changepoints. For well-behaved series, the random walk process, with $D = 1$, allows us to estimate smooth functions for $\{\beta_t\}$ through a small value of σ_{ω}^2 . However, the random walk process has no way of also estimating a discrete processes such as changepoints. As a result, the decoupled approach utilizes a penalized loss function as a secondary step to estimate changepoints. The requirement for the penalized loss in the second step is a relatively smooth estimate of $\{\beta_t\}$. As we will shown later on, for more noisy series, locally adaptive shrinkage priors may be necessary to induce sufficiently smooth estimation.

We fit the above model to the observed data via Gibbs sampling and retrieve posterior estimates for the latent parameters. Let $\{\bar{\beta}_t\}$ denote the posterior mean of the trend estimate from the Bayesian DLM. Since the Bayesian DLM above models heteroskedastic noise, we first consider a weighted least squares loss function: $L_{\lambda}^*(\tilde{\boldsymbol{\beta}}_t) = \sum_{t=1}^n [w_t(y_t - x_t \tilde{\beta}_t)]^2 + q_{\lambda}(\tilde{\boldsymbol{\beta}}_t)$. In the loss, $\tilde{\boldsymbol{\beta}}_t = (\tilde{\beta}_1, \dots, \tilde{\beta}_n)$, $q_{\lambda}(\cdot)$ is a penalty function to induce sparsity given a penalty parameter λ , and $\{w_t\}$ are the weights for each time-step. Details on $q_{\lambda}(\cdot)$ and $\{w_t\}$ will be given in Section 2.2.

One issue with the above loss is that the observed data may contain extreme values or local fluctuations. The observed data may also be subject to influence from potential covariates. Since the goal of the estimator is to produce a simple fit of the true signal $\{\beta_t\}$, we modify the loss by replacing $\{y_t\}$ with its conditional expectation under the Bayesian DLM. This results in the decoupled loss as follows:

$$L_\lambda^*(\tilde{\beta}_t) = \sum_{t=1}^n [w_t(x_t\bar{\beta}_t - x_t\tilde{\beta}_t)]^2 + q_\lambda(\tilde{\beta}_t) \quad (2)$$

Equation 2 can be thought of as a second level shrinkage on the underlying coefficients to induce hard thresholding. The loss function, parametrized by the penalty parameter λ , will be utilized to select changepoints from the posterior estimates of a Bayesian DLM.

2.2 Weights and Penalty Function

The choice of weighted least squares for the loss allows the decoupled approach to utilize estimated variance from the Bayesian DLM to induce additional localized adaptivity. The weights allow the penalty to adjust to regions of high/low volatility inherent in the data, inducing a smaller loss for time-steps with a larger variance and a larger loss for time-steps with a smaller variance.

For the weights $\{w_t\}$, the classic choice is inverse to the noise standard deviation (Kiers, 1997). In our case, since we have a posterior estimate of the noise variance at each time-step through the Bayesian DLM, we set our weights to be

$$w_t = \left\{ \overline{\sigma_{\epsilon,t}^2} \right\}^{-1/2} \quad \text{for } t = 1, \dots, n \quad (3)$$

where $\overline{\sigma_{\epsilon,t}^2}$ is the posterior mean for the variance of time t . As previously discussed, the weights will induce additional robustness for change detection in heteroskedastic data.

The penalty term $q_\lambda(\tilde{\beta})$ will penalize the number time-steps for which the D th difference (i.e. $D = 1$ or 2) in $\tilde{\beta}$ is non-zero. Table 1 shows three possible choices for the penalty function. Ideally, the ℓ_0 penalty will be used to identify the optimal subset of time-steps in which the D th difference are non-zero. However, the ℓ_0 penalty is difficult to estimate efficiently, making it infeasible for long time-series. One solution is to relax the ℓ_0 penalty to the ℓ_1 penalty. However, the ℓ_1 penalty induces shrinkage which tends to bias the result. This is due to the fact the penalty term increases linearly in relation to $\{\Delta^D \tilde{\beta}_t\}$, resulting in the penalty favoring changepoints of low magnitude. As

Table 1: Choices of Penalty Function

	ℓ_0	ℓ_1	Adaptive ℓ_1
Penalty Function	$\lambda \sum_t \mathbb{I}_{\Delta^D \tilde{\beta}_t \neq 0}$	$\lambda \sum_t \Delta^D \tilde{\beta}_t $	$\lambda \sum_t \frac{1}{ \psi_t } \Delta^D \tilde{\beta}_t $
Motivation	Selection	Shrinkage and Selection	Combination of ℓ_0 and ℓ_1

we will shown in the simulations, using the ℓ_1 penalty directly will lead to significant over-estimation of changepoints.

A refined goal is then to identify a penalty function that combines the computational efficiency of the ℓ_1 penalty and the optional subset selection ability of the ℓ_0 penalty. As result, we propose a version of the adaptive ℓ_1 penalty (Zou, 2006) that pushes the ℓ_1 penalty closer to the ℓ_0 penalty. The resulting penalty can be written as follows:

$$q_\lambda(\tilde{\beta}) = \lambda \sum_t \frac{1}{|\psi_t|} |\Delta^D \tilde{\beta}_t| \quad (4)$$

where $\psi_t = \overline{\Delta^D \beta_t}$ for all t . Motivated by similar refinement in Hahn and Carvalho (2015), ψ_t at time t is the posterior mean of the D th degree difference of β_t . This term can function as a normalizer which levels the impact of each changepoint regardless of the magnitude of the change at that time-step. In a time-step with a larger change in $\{\beta_t\}$, ψ_t will tend to be higher in magnitude, leading a changepoint to be penalized less. As a result, this weight term corrects some of the bias in the ℓ_1 penalty and gives better results for changepoint estimation.

2.3 Selecting the Optimal Number of Changepoints

As seen in Equations 2 and 4, we utilize a penalty functions indexed by a penalty parameter λ . As λ approaches 0, there would be no enforcement of sparsity and every point will be treated as a changepoint. As λ approaches ∞ , all $\{\Delta^D \tilde{\beta}_t\}$ will be 0 and no changepoint will be detected. The value of λ plays a critical role in the final selection of the number of changepoints. Typically, with a penalized loss function, cross-validation is used to select the penalty parameter. However, in the case for the proposed decoupled approach, since the loss is taken over the posterior estimate for the latent parameter $\{\beta_t\}$, the MCMC samples can be utilized in identifying the optimal set of changepoints. We propose using the following methodology to select the optimal number of changepoints.

First, minimization of the loss in Equation 2 with our recommended penalty function can be solved via coordinate descent (implemented using R package *glmnet* Friedman *et al.* (2010)) to produce a path of λ values corresponding to different number of changepoints. This path of solutions will express a direct trade-off between goodness-of-fit and the number of changepoints. As the number of changepoints increases, the estimated solution $\tilde{\boldsymbol{\beta}}$ will be fit closer to the posterior mean across time.

Second, for each λ in the corresponding solution path, we will compute the “projected posterior” (Woody *et al.*, 2020) to quantify its uncertainty. The key idea behind the projected posterior is to project each MCMC draw from the Bayesian model onto the summary space defined by locations of changepoints. For a given value λ , let η denote the time indices which $\{\Delta^D \tilde{\beta}_t \neq 0\}$ (i.e. the estimated changepoint locations). Initial points $1, \dots, D$ are automatically included in every η as they are unpenalized. Let $\boldsymbol{\beta}^{(i)}$ denote the i th MCMC draw from the Bayesian model and \mathbf{Z} denote the inverse of the D th difference matrix. For $D = 1$ or 2 , \mathbf{Z} is defined as:

$$D = 1 : \mathbf{Z} = \begin{bmatrix} 1 & 0 & 0 & \cdots & 0 & 0 & 0 \\ -1 & 1 & 0 & \cdots & 0 & 0 & 0 \\ 0 & -1 & 1 & \cdots & 0 & 0 & 0 \\ \vdots & \vdots & \vdots & \ddots & \vdots & \vdots & \vdots \\ 0 & 0 & 0 & \cdots & -1 & 1 & 0 \\ 0 & 0 & 0 & \cdots & 0 & -1 & 1 \end{bmatrix}^{-1} \quad D = 2 : \mathbf{Z} = \begin{bmatrix} 1 & 0 & 0 & \cdots & 0 & 0 & 0 \\ 0 & 1 & 0 & \cdots & 0 & 0 & 0 \\ 1 & -2 & 1 & \cdots & 0 & 0 & 0 \\ \vdots & \vdots & \vdots & \ddots & \vdots & \vdots & \vdots \\ 0 & 0 & 0 & \cdots & -2 & 1 & 0 \\ 0 & 0 & 0 & \cdots & 1 & -2 & 1 \end{bmatrix}^{-1}.$$

Let \mathbf{Z}_η denote the subset of columns of \mathbf{Z} indexed by a given η . The i th projected posterior is then given by:

$$\boldsymbol{\beta}_\eta^{(i)} = (\mathbf{Z}_\eta^\top \mathbf{Z}_\eta)^{-1} \mathbf{Z}_\eta^\top \boldsymbol{\beta}^{(i)}$$

where \mathbb{T} is the transpose operator. This projects $\boldsymbol{\beta}^{(i)}$ from each MCMC draw onto the best fitted model given the changepoint estimates. In summary, the “projected posterior” takes a set of changepoint locations and produces the best estimate of $\boldsymbol{\beta}$ for each of the MCMC draws given the changepoint locations. This, in turn, allows us to visualize a trade-off between the number of changepoints and the corresponding fit for the posterior estimates.

Third, after deriving the projected posterior, we need a diagnostic tool to calculate goodness-of-fit. A common criterion for model selection is the amount of variation explained. Since we accounted for heteroskedasticity in the noise term of the Bayesian DLM, we propose using the

following metric as an estimate for amount of variation explained by the changepoints for the i th MCMC draw:

$$R_\eta^{2,(i)} \equiv 1 - \frac{\sum_{t=1}^n (w_t^{1/2} (x_t \beta_t^{(i)} - x_t \beta_{\eta,t}^{(i)}))^2}{\sum_{t=1}^n (w_t^{1/2} (x_t \beta_t^{(i)} - x_t \mu_{\beta^{(i)}}))^2}$$

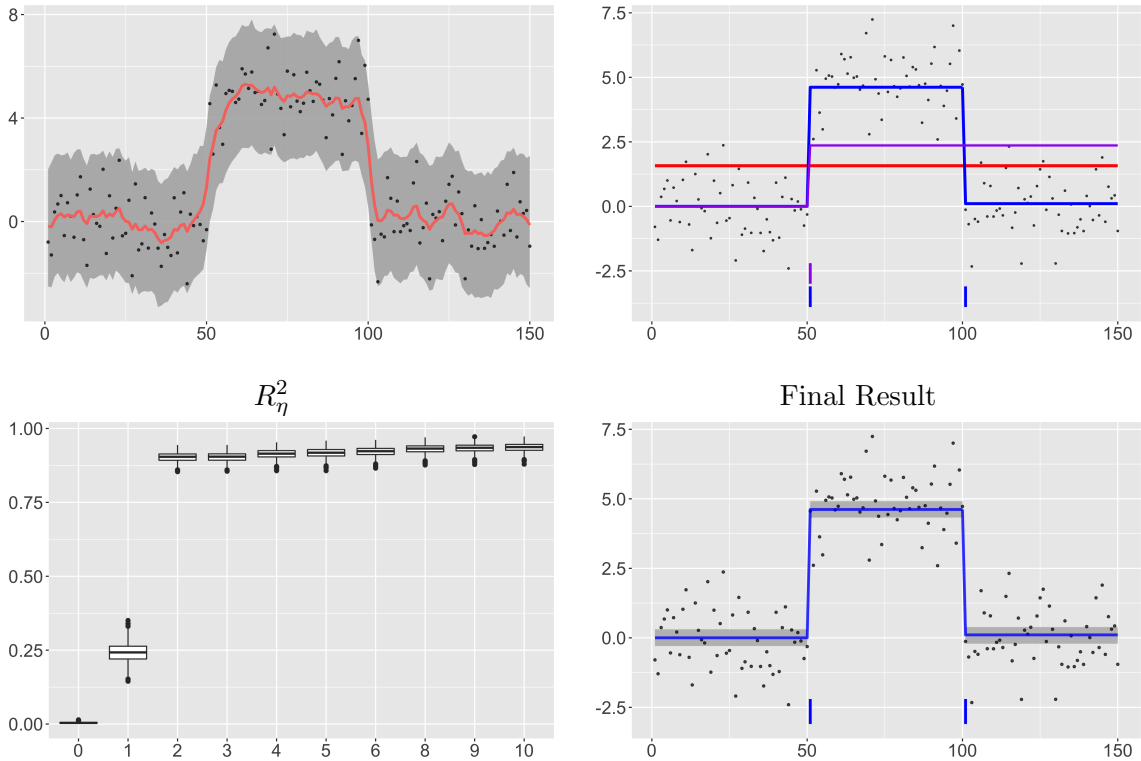
where $\mu_{\beta^{(i)}}$ is the mean over t of the i th MCMC draw, $\beta^{(i)}$. This metric is similar to R-squared in that it measures the amount of variation explained by the projected posterior β_η for each of the MCMC draws. However, error for each time-step is multiplied by the corresponding weight value, giving time-steps with higher variances lower weights. This makes sense as we expect more uncertainty in regions of high noise volatility. In turn, this metric provides an estimate of variation explained for each of the MCMC draws. The higher the value of $R_\eta^{2,(i)}$, the better the fit of the “projected posterior” for the i th MCMC draw. For selecting the optimal value of λ , we will select the lowest number of changepoints which the upper 90% credible interval for $\tilde{E}[R_\eta^2]$ exceeds a certain threshold. We find this simple selection criterion to be quite effective in empirical settings and easy to visualize. Details on the threshold selection will be given in Section 3.

Figure 1 shows an example of the decoupled approach on simulated series with two changepoints in mean. The top-left plot shows the fit from a Bayesian DLM with random walk. While the fit is very wiggly, the model captures the underlying trend for the most part. However, the model does not provide a clear identification of changepoints. The projected posterior for varying number of changepoints is shown in the top-right plot. For 0 changepoints, the projected posterior just fits the mean. For 1 changepoint, the projected posterior fits the first segment and blends the next 2 segments. For 2 changepoints, the projected posterior captures both changepoints. This is reflected in goodness-of-fit R_η^2 . The metric shows large jumps from 0 to 1 changepoints and 1 to 2 changepoints, with marginal improvements afterward. We select 2 changepoints as the final result and plot the final projected posterior in the bottom-right plot. As seen, we can turn a very wiggly fit of the Bayesian DLM to a clear separation of drifts vs shifts.

2.4 Locally Adaptive Trends with Global-Local Shrinkage Priors

In the current model, we assume the coefficients $\{\beta_t\}$ follows a random walk with a constant variance σ_ω^2 . While this setup can be sufficient for data with strong signal, this model tends overfit in datasets with low signal-to-noise ratios. Previous work have found shrinkage priors reduces overfitting and improve the performance of Bayesian dynamic linear models (Kowal *et al.*, 2019;

Figure 1: Illustrative Example of the Decoupled Approach with Random Walk Bayesian DLM



The top-left plot shows the resulting posterior mean of $\{\beta_t\}$ using a Bayesian DLM with random walk. 90% credible bands are shown in dark gray. The top-right plot shows the mean of the projected posterior for 0, 1, and 2 number of changepoints. The bottom-left plots shows the distribution of R_η^2 as a function of the number of changepoints. The bottom-right plots shows the final resulting fit from the decoupled approach with 90% credible bands.

Wu and Matteson, 2020; Belmonte *et al.*, 2013; Banbura *et al.*, 2010). Shrinkage priors present a trade-off between goodness-of-fit and smoothness of the underlying process; a stronger shrinkage prior will typically result in a smoother underlying fit for the $\{\beta_t\}$ process. In this section, we will introduce the use shrinkage priors for the decoupled approach.

As previous discussed in Section 1, various forms of shrinkage priors have shown to be effective in Bayesian DLMs. For this section, we will focus on the class of so called “global-local shrinkage priors” which have shown to be effective for Bayesian modeling (Bhadra *et al.*, 2016). Equation 1

will be modified to be as follows:

$$\begin{aligned}
 y_t &= x_t \beta_t + \epsilon_t, & \epsilon_t &\sim N(0, \sigma_{\epsilon,t}^2) \\
 \Delta^D \beta_t &= \omega_t & \omega_t &\sim N(0, \tau_\omega^2 \gamma_{\omega,t}^2)
 \end{aligned}
 \tag{5}$$

This extension induces global-local shrinkage on the D th difference of the coefficients for the predictor. The parameter τ_ω^2 induces global shrinkage across all time-steps and the process $\{\gamma_{\omega,t}^2\}$ induces time-specific shrinkage for the coefficients at each time-step. The two parameters combined together shrink small deviations toward zero while allowing large signals to remain unchanged. This provides localized adaptivity while maintaining strong global shrinkage. One example of such shrinkage prior is the dynamic shrinkage process detailed in [Kowal and Bourgeois \(2020\)](#). The shrinkage process is detailed as follows:

$$h_t \equiv \log(\tau_\omega^2 \gamma_{\omega,t}^2), \quad h_t = u + \phi(h_{t-1} - u) + \xi_t,
 \tag{6}$$

where $\xi_t \stackrel{iid}{\sim} Z(0.5, 0.5, 0, 1)$, in which $Z(\cdot)$ denotes the four parameter Z -distribution. Due to the effectiveness of the model shown in the paper, we will utilize this model for all simulations and call this version of the decoupled approach: decoupled dynamic shrinkage (DC-DS). Note that the decoupled approach is not restricted to the choice of shrinkage priors, other global-local shrinkage priors such as the double-gamma, double-exponential priors will achieve similar performances.

One major advantage for the decoupled approach is that the choice of shrinkage priors on the $\{\beta_t\}$ process does not affect the second step of the decoupled analysis. As a result, a highly complex shrinkage framework can be fit onto the existing data. The decoupled approach only utilizes the posterior estimates of $\{\beta_t\}$ in the second step for changepoint selection. As we will shown in the simulations, the resulting smoother estimate of the $\{\beta_t\}$ process from incorporation of shrinkage priors will reduce over-estimation and improve the selection of changepoints. Examples of results are shown in [Sections 3.1 and 4](#).

2.5 Multiple Time Varying Linear Predictors

In this section, we will extend the decoupled approach to deal with multiple predictors. Changepoint detection in multiple linear regression can be a challenging problem as coefficients of different predictors may have changepoints at different time-steps. Most existing work in this area focus on

identifying changepoint jointly across series and lack the ability to identify predictors associated with each changepoint. To accommodate for additional flexibility, we allow the users to specify any type of group structure among predictor series. All predictor series in the same group are assumed to have the same changepoints. For example, if we wish to identify changepoint separately for each individual predictor, then we can place all predictors in its own group and identify changes separately. On the other hand, if we wish to identify joint changepoints across all predictor series, then we can place all predictors in one group. By separating the process of modeling and changepoint selection, the decoupled approach allows for creation of any subset of groupings for selection without affecting the modeling of the Bayesian DLM. This additional flexibility can provide great insights on which predictor series is changing over time.

The details for the updated model can be seen as follows. Suppose now we have p predictor series $\mathbf{X} = \text{blockdiag}(\mathbf{x}'_1, \dots, \mathbf{x}'_n)$ where \mathbf{X} is a block-diagonal matrix with row i containing \mathbf{x}'_i on the block-diagonal. Let $\mathbf{x}_i = (x_{i,1}, \dots, x_{i,p})'$, we can rewrite Equation 1 as follows:

$$\begin{aligned} y_t &= \mathbf{x}'_t \boldsymbol{\beta}_t + \epsilon_t, & \epsilon_t &\sim N(0, \sigma_{\epsilon,t}^2) \\ \Delta^D \boldsymbol{\beta}_t &= \boldsymbol{\omega}_t & \boldsymbol{\omega}_t &\sim N(\mathbf{0}, \boldsymbol{\Sigma}_{\boldsymbol{\omega},t}) \end{aligned} \quad (7)$$

In comparison to Equation 1, the model now involves p predictor series at each time-step. The variance is modeled by a heteroskedastic process $\{\sigma_{\epsilon,t}^2\}$ and the D th difference for $\{\boldsymbol{\beta}_t\}$ is assumed to be normal with mean $\mathbf{0}$ and variance $\boldsymbol{\Sigma}_{\boldsymbol{\omega},t}$. Equation 7 provides a framework which works well for a wide range of Bayesian DLMs. For the simulations and real world analysis, we assume $\boldsymbol{\Sigma}_{\boldsymbol{\omega},t}$ is diagonal with a dynamic shrinkage priors on each diagonal term. However, the decoupled approach will also work with other structures for this variance matrix. Once the above model is fit and MCMC samples are estimated, the decoupled loss for multiple predictor series can be written as follows:

$$\begin{aligned} L_\lambda(\tilde{\boldsymbol{\beta}}) &= \|\mathbf{W}(\mathbf{X}\tilde{\boldsymbol{\beta}} - \mathbf{Y})\|_2^2 + q_\lambda(\tilde{\boldsymbol{\beta}}) \\ q_\lambda(\tilde{\boldsymbol{\beta}}) &= \lambda \sum_{t=1}^n \sum_{g=1}^G \frac{1}{|\psi_{g,t}|} |\Delta^D \boldsymbol{\beta}_{g,t}| \end{aligned} \quad (8)$$

where $\tilde{\boldsymbol{\beta}} = \text{vec}(\tilde{\boldsymbol{\beta}}_1, \dots, \tilde{\boldsymbol{\beta}}_n)'$ and \mathbf{W} is a diagonal matrix filled by weights seen in Equation 3. The penalty function $q_\lambda(\tilde{\boldsymbol{\beta}})$ is a variation of grouped lasso (Yuan and Lin, 2007) where G is the number of groups, $|\Delta^D \boldsymbol{\beta}_{g,t}|$ is the sum of absolute value of D th difference of all series in the particular

group and $|\psi_{g,t}|$ is the average sum of weight for data in each group. Similar to Equation 4, the term $|\psi_{g,t}|$ functions as a normalizer across different groups to adjust for the number of predictor series and the magnitude of change. We illustrate the effectiveness of the decoupled approach for dealing with multiple linear predictors in Section 3.2.1 and 3.2.2.

2.6 Incorporating Static Parameters into Changepoint Analysis

Another important element to consider for Bayesian DLMS is the existence of static variables aka non-time-varying covariates. Since these covariates have non-time-varying relation with the response variable, we are not interested in identifying changepoints associated with these covariates. Rather, we wish to fit a model for our predictors with these covariates included and identify changes in relationship between the predictors and the response. Suppose we have a set of l covariates denoted by $\mathbf{Z} = (\mathbf{z}_1, \dots, \mathbf{z}_n)$ where $\mathbf{z}_i = (z_{i,1}, \dots, z_{i,l})'$ for $i = 1, \dots, n$. The Bayesian DLM, modified from Equation 7 can be written as follows:

$$\begin{aligned} y_t &= \mathbf{x}'_t \boldsymbol{\beta}_t + \boldsymbol{\alpha}' \mathbf{z}_t + \epsilon_t, & \epsilon_t &\sim N(0, \sigma_{\epsilon,t}^2) \\ \Delta^D \boldsymbol{\beta}_t &= \boldsymbol{\omega}_t & \boldsymbol{\omega}_t &\sim N(0, \boldsymbol{\Sigma}_{\omega,t}) \end{aligned} \quad (9)$$

where $\boldsymbol{\alpha} = (\alpha_1, \dots, \alpha_l)'$ are the estimated coefficients for these covariates. This model can be estimated using standard Bayesian methodology for DLMS. Once the posterior estimates are derived, we combine \mathbf{X} and $\boldsymbol{\alpha}$ for the decoupled loss as follows:

$$L_\lambda(\tilde{\boldsymbol{\beta}}, \tilde{\boldsymbol{\alpha}}) = \|\mathbf{W}([\mathbf{X}, \mathbf{Z}][\tilde{\boldsymbol{\beta}}', \tilde{\boldsymbol{\alpha}}']' - [\mathbf{X}, \mathbf{Z}][\tilde{\boldsymbol{\beta}}', \tilde{\boldsymbol{\alpha}}']')\|_2^2 + q_\lambda(\tilde{\boldsymbol{\beta}}) \quad (10)$$

where $[\cdot, \cdot]$ denote concatenation of two matrices among columns. Using same notation as previous, \mathbf{X} is a block-diagonal matrix where row i contains \mathbf{x}'_i on the block-diagonal and $\tilde{\boldsymbol{\beta}} = \text{vec}(\tilde{\boldsymbol{\beta}}_1, \dots, \tilde{\boldsymbol{\beta}}_T)^T$. In Equation 10, $\mathbf{X} \in R^{T \times Tp}$, $\mathbf{Z} \in R^{T \times l}$ and $[\mathbf{X}, \mathbf{Z}]$ results in a matrix of dimension $T \times (Tp + l)$ and $[\tilde{\boldsymbol{\beta}}', \tilde{\boldsymbol{\alpha}}']'$ results in a matrix of dimension $(Tp + l) \times 1$. $q_\lambda(\tilde{\boldsymbol{\beta}})$ is the same as Equation 8.

One key note is that the penalty function $q_\lambda(\tilde{\boldsymbol{\beta}})$ does not change with incorporation of these covariates. This is due to the fact that these covariates' relationship with the response do not change over-time and therefore are not penalized. If there exist a large number of these covariates, variable selection can be done by penalizing the ℓ_1 norm of the coefficients $\boldsymbol{\alpha}$. However, as the focus

of this paper is on changepoint analysis, we will not investigate into this further and will leave the covariates unpenalized in the decoupled loss for the rest of the paper. The decoupled loss can be estimated using package for solving grouped lasso such as R package *gglasso*.

The existence of time-varying and non-time-varying covariates have traditionally posed a significant challenge for changepoint analysis in regression. The decoupled approach’s ability to deal with time-varying and non-time-varying covariates grants the algorithm additional flexibility and robustness to deal with various types of real world problems. This extension further highlights the benefit of separating the processes of modeling and changepoint selection. During the modeling step, a complex Bayesian model can be fit to the existing data that incorporates a variety of complexities such as covariates, heteroskedastic noise and non-stationary inputs. As long as the model can produce fairly smooth estimate of the coefficients for the predictors of interest, the decoupled approach can adapt the inference part to identify key changepoints. This level of flexibility grants the decoupled approach the ability to work with more applications than previous existing changepoint algorithms. Examples of the decoupled approach with static parameters can be seen in Section 3.2.3.

3 Simulated Experiments

3.1 Change in Mean in Noisy Environment

In this section, we illustrate the effectiveness and flexibility of the decoupled approach by comparing our method against two other changepoint methods based on penalized likelihood functions. The competing methods are the Pruned Exact Linear Time method (PELT, [Killick *et al.*, 2012](#)) and Robust FPOP algorithm (R-FPOP, [Fearnhead and Rigail, 2019](#)). PELT identifies changepoint based on penalized cost function using a goodness-of-fit metric based on maximum negative likelihood for each segment and a penalty parameter on the number of changepoints. R-FPOP adapts the penalty function using a biweight-loss in order to deal with outliers by establishing a maximum threshold for the impact of each time-step.

We chose these two methods as they are similar to the decoupled approach in their utilization of penalized cost function for identification of changepoints. However, unlike the decoupled approach, they utilize the data rather than posterior from a Bayesian DLM in their penalized loss function. By comparing the decoupled approach against these methods, we will illustrate the benefits of using Bayesian modeling as first step before penalized loss. The comparisons will start on simple

cases of changes in mean with Gaussian noise, then extend to more complicated scenarios adding in outliers and heterogeneity. For both competing methods, we will use the default parameters as utilized in the original papers. For the decoupled approach, we use a cutoff threshold for 0.9 for lowest number of changepoints which the upper 90% credible interval for R_{η}^2 exceeds. Full detail of the parameters used for the Bayesian DLM is shown in the Online Appendix.

Five metrics are used to evaluate the results: Rand index, adjusted Rand index, precision, recall and F1-score. Rand index calculates a similarity score between the predicted partition and the true partition; the score ranges between 0 and 1 with 1 being a perfect match. Adjusted Rand index provides an additional correction step to the Rand Index by accounting for random chance of a correct partition. Precision measures proportion of true changepoints in the number of predicted changepoints while recall measures proportion of all true changepoints detected by the models. F1-score calculates the harmonic mean between precision and recall. Since changepoints occur very rarely in the data, the F1-score is a good indicator for the accuracy of predictions (van den Burg and Williams, 2020). We consider a predicted changepoint to be a true positive if it is within ± 5 of a true changepoint, with the caveat that each true changepoint can only match to at most one predicted changepoint.

3.1.1 Change in Mean with Gaussian Noise

For the first set of simulations, we start with a simple change in mean with standard Gaussian noise. We simulate data of length 200, with a changepoint in the middle of the data at location 100. We adjust different levels for the magnitude of change to understand the effectiveness of the algorithms with varying signal-to-noise ratios. We test 4 different magnitudes of change values of $\{1, 0.75, 0.5, 0.25\}$. We will compare the decoupled approach with random walk (DC-RW, model introduced in Section 2.1) and the decoupled approach with dynamic shrinkage (DC-DS, model introduced in Section 2.4) against PELT. PELT is a penalized likelihood changepoint algorithm which is designed to identify changes in this setting, making it a good baseline for comparison. We expect the decoupled approach to perform slightly worse than PELT in this setting as a trade-off for increased flexibility. As we will show in the later simulations, the flexibility of the decoupled approach allows it to perform much better when the assumptions of homoskedasticity and Gaussian noise are violated.

As seen in Table 2, the decoupled approach with dynamic shrinkage performs slightly worse than PELT. With a signal-to-noise ratio of 1 to 1 (magnitude of change 1), both DC-DS and PELT

Table 2: Single Change in Mean

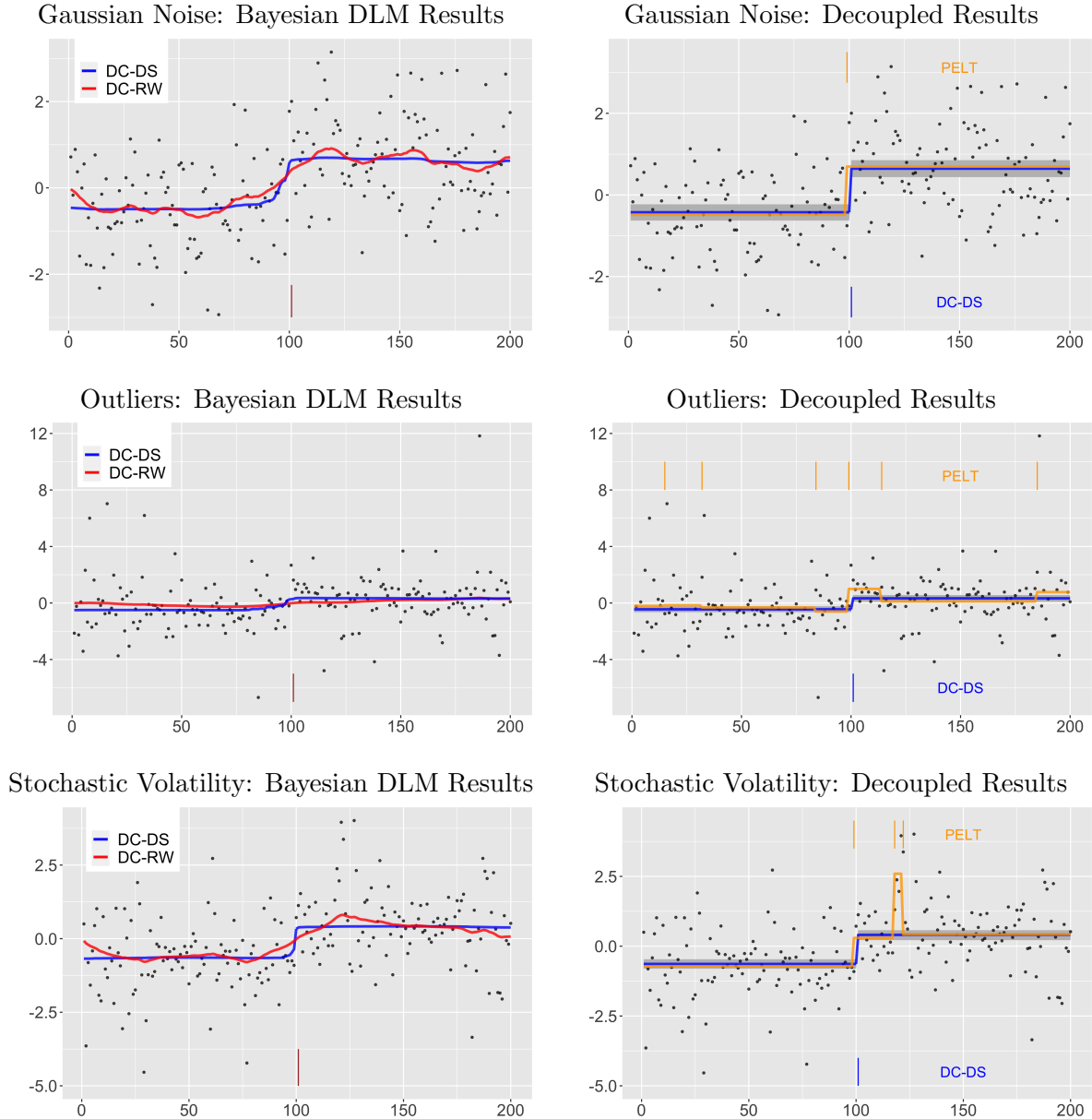
Mag. of Change	Algorithms	Rand Avg.	Adj. Rand Avg.	Precision	Recall	F1-score
1	DC-RW	0.795 _(0.013)	0.590 _(0.027)	0.18	0.83	0.29
	DC-DS	0.964 _(0.004)	0.929 _(0.009)	0.78	0.83	0.80
	PELT	0.968 _(0.004)	0.936 _(0.007)	0.82	0.87	0.84
0.75	DC-RW	0.689 _(0.016)	0.379 _(0.031)	0.14	0.53	0.22
	DC-DS	0.926 _(0.009)	0.851 _(0.018)	0.68	0.56	0.61
	PELT	0.930 _(0.009)	0.860 _(0.021)	0.62	0.67	0.64
0.5	DC-RW	0.576 _(0.012)	0.156 _(0.024)	0.12	0.25	0.16
	DC-DS	0.791 _(0.017)	0.582 _(0.035)	0.23	0.38	0.29
	PELT	0.755 _(0.021)	0.512 _(0.041)	0.38	0.30	0.33
0.25	DC-RW	0.498 _(0.000)	0.000 _(0.000)	0.00	0.00	0.00
	DC-DS	0.510 _(0.006)	0.025 _(0.013)	0.02	0.01	0.01
	PELT	0.498 _(0.000)	0.000 _(0.000)	0.00	0.00	0.00

Table details results of the decoupled approach with random walk, decoupled approach with dynamic shrinkage, and PELT on simulated data with one change in mean of varying magnitudes and standard Gaussian noise. Rand average and adjusted Rand average measures the similarity between predicted partition and true partition. Standard error for Rand average and adjusted Rand average are given in subscripts. F1-score measures accuracy of changepoint detection through a comparison of precision and recall.

perform similarly well with Rand average above 0.95, adjusted Rand average above 0.925 and F1-score above 0.8. As the signal-to-noise ratio reaches a low of 1 to 4 (magnitude of change 0.25), both changepoint algorithms can no longer distinguish the correct changepoint. For the magnitude change of 0.75 and 0.5, PELT performs slightly better in terms of F1-score. However, we still see a trade-off of precision and recall between the two algorithms. For magnitude of change of 0.5, PELT has a higher precision while DC-DS has a higher recall. This shows that DC-DS has a tendency to slightly over-predict in low signal-to-noise ratio while PELT has a tendency to under-predict. A key note is that DC-DS maintains the highest Rand and adjusted Rand average in this settings, showing that DC-DS produces the partition closest to the true partition.

Comparing DC-RW against DC-DS, we can clearly see that using shrinkage priors in the Bayesian DLM significantly improves the performance of the decoupled approach. This is due to the fact that shrinkage priors induce smoother estimates of the underlying trend; as a result, changepoint inference on the posterior becomes much easier. This further supports the discussion in Section 2.4 of the advantages of the decoupled framework by allowing for fitting of a highly complex shrinkage framework. Due to the significant improvements of using shrinkage priors in the baseline case, we will use DC-DS as our main method from this point onward.

Figure 2: Example Plot for Decoupled Analysis of Change in Mean



The top-left, mid-left and bottom-left plots show posterior mean of Bayesian DLMs fit on data with Gaussian Noise, t-distributed noise and stochastic volatility respectively. The blue line is the posterior mean for fit with dynamic shrinkage (DC-DS) while the red line is posterior mean for fit with random walk (DC-RW). The brown vertical bar indicate the correct changepoint location. As seen, the addition of shrinkage priors induce smoother estimates for the $\{\beta_t\}$ process. The top-right, mid-right and bottom-right plot shows posterior mean (blue line) of the optimal decoupled result for DC-DS on the same data as left-side with 95 percent credible bands in dark gray. The correct changepoint is shown by the brown vertical bar.

Table 3: Change in Mean with Outliers

Mag. of Change	Algorithms	Rand Avg.	Adj. Rand Avg.	Precision	Recall	F1-score
2	DC-DS	0.977 _(0.003)	0.954 _(0.007)	0.88	0.91	0.89
	PELT	0.681 _(0.006)	0.361 _(0.012)	0.06	0.82	0.11
	R-FPOP	0.952 _(0.011)	0.904 _(0.022)	0.86	0.83	0.84
1.5	DC-DS	0.967 _(0.005)	0.934 _(0.009)	0.80	0.82	0.81
	PELT	0.689 _(0.007)	0.376 _(0.014)	0.05	0.74	0.10
	R-FPOP	0.860 _(0.020)	0.721 _(0.040)	0.80	0.63	0.70
1	DC-DS	0.935 _(0.007)	0.870 _(0.015)	0.68	0.60	0.63
	PELT	0.680 _(0.007)	0.358 _(0.013)	0.04	0.59	0.08
	R-FPOP	0.804 _(0.009)	0.638 _(0.019)	0.35	0.62	0.44
0.5	DC-DS	0.742 _(0.018)	0.486 _(0.036)	0.18	0.32	0.24
	PELT	0.676 _(0.006)	0.350 _(0.013)	0.04	0.48	0.07
	R-FPOP	0.741 _(0.017)	0.484 _(0.035)	0.15	0.25	0.19

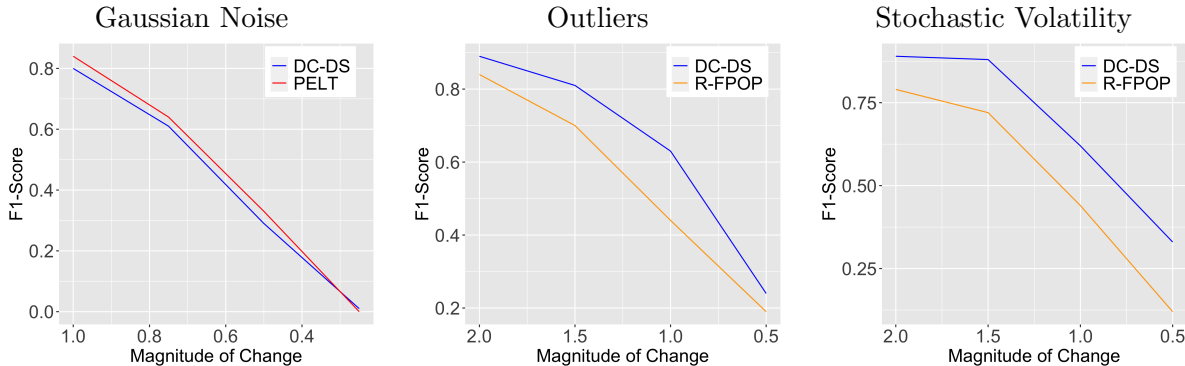
Table details results of DC-DS, PELT and R-FPOP on simulated data with one change in mean of varying magnitude of change and outliers. Outliers are simulated using t-distributed noise with 2 degrees of freedom.

3.1.2 Change in Mean with Outliers

For this set of simulations, we added outliers onto the same problem as Section 3.1.1 to illustrate how the performance of these algorithms change in the presence of outliers. We will add the R-FPOP method to the comparison as this method is designed to identify changepoints in presence of outliers. The simulation setting will be kept the same as Section 3.1.1; 100 simulation will be generated of data of length 200 with various magnitude of changes. As this is a significantly more difficult problem, we increase the magnitude of change to be selected from $\{2, 1.5, 1, 0.5\}$. Instead of Gaussian noise, we will utilize t-distributed noise with 2 degrees to simulate data with extreme outliers.

The results of the simulation can be seen in Table 3. With the addition of outliers, the decoupled approach is able to achieve the best performance across all settings. By utilizing a Bayesian DLM with dynamic shrinkage, the decoupled approach is robust to the presence of extreme outliers. PELT, with no mechanism to deal with extreme values, are significantly influenced by outliers. This lead to PELT to significantly over-predict the number of changepoints. To be fair to PELT, the algorithm is not intended to work on datasets with outliers. In the setting of magnitude of change of 2, DC-DS achieves an F1-score of 0.89 in comparison to 0.84 for R-FPOP. As the signal-to-noise ratio decreases, we can see an increasing gap in adjusted Rand average and F1-score between DC-DS and R-FPOP. This indicates that DC-DS can produce more precise changepoint

Figure 3: Change in Mean: Comparison of F1-Scores



F1-score calculates the harmonic mean between precision and recall. The score ranges between 0 and 1 with 1 being a perfect prediction. The left plot shows F1-score of DC-DS (blue line) against PELT (red line) in simulated data with Gaussian noise from Section 3.1.1. The middle plot shows F1-score of DC-DS (blue line) against R-FPOP (orange line) in simulated data with outliers from Section 3.1.2. The right plot shows F1-score of DC-DS (blue line) against R-FPOP (orange line) in simulated data with stochastic volatility from Section 3.1.3.

estimations and more accurate partitions. The advantage becomes more significant in the setting of magnitude of change of 1. DC-DS achieves a F1-score of 0.63 in comparison to 0.44 of R-FPOP. As magnitude of change approaches 0.5, the problem becomes too difficult for all algorithms and F1-scores are very low.

Figure 2 illustrates the results of the decoupled approach in three example series generated with Gaussian noise, t-distributed noise and stochastic volatility. The blue line in the middle-left plot shows the posterior mean of the $\{\beta_t\}$ process from a Bayesian dynamic linear model with dynamic shrinkage on a series generated with outliers. The middle-right plot then shows the optimal fit from the decoupled loss and the resulting projected posterior. This highlights one major advantage of separating shrinkage and changepoint selection. Despite the presence of outliers, a Bayesian DLM with dynamic shrinkage is able to predict a relatively smooth underlying trend with one jump around the changepoint location. The decoupled loss then identifies the optimal piece-wise constant fit to the smooth posterior and flags the correct changepoint location.

3.1.3 Change in Mean in Presence of Heteroskedasticity

For the next set of simulations, we evaluate these algorithms in presence of heterogeneity. We simulate 100 series of length 200, with a changepoint in the middle of the data at location 100. However, instead of standard Gaussian noise or t-distributed noise, we generate noise using stochas-

Table 4: Change in Mean with Heterogeneity

Mag. of Change	Algorithms	Rand Avg.	Adj. Rand Avg.	Precision	Recall	F1-score
2	DC-DS	0.982 _(0.004)	0.964 _(0.008)	0.89	0.90	0.89
	PELT	0.834 _(0.010)	0.667 _(0.019)	0.11	0.96	0.20
	R-FPOP	0.944 _(0.009)	0.889 _(0.018)	0.73	0.85	0.79
1.5	DC-DS	0.977 _(0.004)	0.955 _(0.008)	0.87	0.90	0.88
	PELT	0.827 _(0.010)	0.654 _(0.020)	0.10	0.89	0.19
	R-FPOP	0.926 _(0.011)	0.852 _(0.022)	0.64	0.81	0.72
1	DC-DS	0.931 _(0.009)	0.862 _(0.020)	0.60	0.64	0.62
	PELT	0.800 _(0.010)	0.599 _(0.020)	0.07	0.61	0.13
	R-FPOP	0.835 _(0.019)	0.671 _(0.037)	0.39	0.50	0.44
0.5	DC-DS	0.836 _(0.015)	0.673 _(0.030)	0.29	0.38	0.33
	PELT	0.686 _(0.013)	0.373 _(0.026)	0.03	0.25	0.05
	R-FPOP	0.626 _(0.018)	0.254 _(0.036)	0.12	0.11	0.12

Table details results of DC-DS, PELT and R-FPOP on simulated data with one change in varying magnitude and stochastic volatility. Stochastic volatility is simulated using highly autocorrelated SV(1) model.

tic volatility of order 1 (Kim *et al.*, 1998) as follows:

$$\log(\sigma_{\epsilon,t}^2) = \mu_\epsilon + \phi_\epsilon[\log(\sigma_{\epsilon,t-1}^2) - \mu_\epsilon] + \xi_{\epsilon,t}, \quad \xi_{\epsilon,t} \sim N(0, \sigma_\eta^2). \quad (11)$$

We set the following values: $\mu_\epsilon = 0$, $\phi_\epsilon = 0.9$, and $\sigma_{\epsilon,t}^2 = 0.5$. This creates high auto-correlation which causes regions of high/low volatility which can occur frequently in real world data. We utilized 4 magnitude of change values of $\{0.5, 1, 1.5, 2\}$ to evaluate the algorithms' effectiveness in varying signal-to-noise ratios. The results are reported in Table 4. To be fair to PELT and R-FPOP, the algorithms are not intended to work in this setting. As a result, the performances are not reflective of the effectiveness of the algorithms. Rather, this illustrates the flexibility of the decoupled approach in being able to utilize Bayesian DLMS to locally adapt to heterogeneity inherent in datasets.

Comparing results in Table 4 to Table 2 for magnitude of change 1, we see that the performance of all changepoint algorithms decreased in presence of stochastic volatility. This is to be expected as stochastic volatility makes detection of changepoints much more difficult. With the addition of stochastic volatility, DC-DS outperformed other competing changepoint methods in all settings. DC-DS achieves a F1-score of 0.89 for setting of magnitude of change of 2, a F1-score of 0.62 for setting of magnitude of change of 1 and a F1-score of 0.33 for setting of magnitude of change of 0.5. DC-DS achieves the most accurate partitions by having the highest adjusted Rand average and

the best trade-offs of precision/recall. This illustrates the robustness of the decoupled approach in dealing with heterogeneity.

Figure 3 summarizes the results in term of F1-score for Section 3.1. As seen in the plots, the decoupled approach is slightly worse in standard Gaussian noise setting but performs significantly better when outliers or stochastic volatility are added. This illustrates the trade-off of the decoupled approach. By fitting a Bayesian DLM to the data first, the decoupled approach can be more locally adaptive to the complexities inherent in time series data. Outliers and heterogeneity are just two examples of the challenges that the decoupled approach can deal with. As long as the posterior estimates for the $\{\beta_t\}$ process remains relatively smooth, the decoupled loss can identify correct changepoint locations in a variety of complex scenarios.

3.2 Change in Regression

For the next sets of experiments, we will examine the effectiveness of the decoupled approach in various regression situations. In particular, we will look at three different situations associated with changes in relationship between predictors and response. First, we will look at the case of multiple predictors with two changepoints and constant variance. Next, we will extend the analysis for data with stochastic volatility. Finally, we will examine the case with added covariates.

A tremendous amount of work has been done using variations of the lasso penalty for identifying changepoints in linear regression (Ciuperca and Maciak, 2019; Jin *et al.*, 2016; Qian and Su, 2016; Ciuperca, 2014). We will compare against the algorithm SGL based sparse group lasso penalty (Zhang *et al.*, 2015) as it closest resembles the decoupled loss. In addition, we will compare against two other regression changepoint algorithms: variance projected wild binary segmentation denoted by VPWBS (Wang *et al.*, 2021) and a method called computationally efficient change point detection which we will denote by CECPD (Leonardi and Bühlmann, 2016). VPWBS projects the predictors onto a univariate series and then utilizes wild binary segmentation to identify the changepoints. CECPD uses a combination of binary segmentation and dynamic programming to estimate the optimal set of changepoints that minimizes a ℓ_1 loss function. We use default parameters for CECPD as recommended in the original paper. For VPWBS and SGL, we utilize cross-validation to select the optimal parameters.

Out of the three methods, SGL is the closest related to our method as it utilizes a sparse group lasso penalty that penalizes for number of changepoints as well as goodness of fit within each segment. However, there are two key differences between the decoupled loss and SGL. First, the

decoupled approach does not use cross-validation to select the optimal penalty parameter. Instead, the penalty selection criterion introduced in Section 2.3 is used to select optimal changepoint locations. Second, a normalizer ($\{\psi_{g,t}\}$) based on posterior average magnitude of change is utilized in the penalty term for the decoupled approach. As we will show throughout this section, these differences induce more robustness and better performance for the decoupled approach. The same metrics introduced in Section 3.1 will be used to evaluate the performance of the methods.

3.2.1 Change in Regression for Multiple Predictors

For the first set of simulations, we examine the cases of multiple predictors with two joint changepoints. This is a standard case for changepoint analysis in regression setting and can be used as a baseline for comparison. We perform 100 simulations to generate data of length 300 with two changepoints at location 75 and 225. The response series $\{y_t\}$ and the predictor series $\{\mathbf{x}_t\}$ where $\mathbf{x}_t = (x_{t,1}, x_{t,2}, x_{t,3})$ are generated with the following relationship:

$$y_t = \begin{cases} \beta'_1 \mathbf{x}_t + \epsilon_t & t \leq 74 \\ \beta'_2 \mathbf{x}_t + \epsilon_t & 75 \leq t \leq 224 \\ \beta'_1 \mathbf{x}_t + \epsilon_t & t \geq 225 \end{cases}$$

where $\{\epsilon_t\}$ is a standard Gaussian noise, $(\beta_1, \beta_2) = (0, C)$ where C denotes the magnitude of change. As change in regression tends to be more difficult than change in mean, the magnitude of change will be higher in the coefficients. We will select C from the following set: $\{2, 1, 0.5\}$. The predictors are generated from $\mathbf{x}_t \sim_{i.i.d.} N(0, \mathbf{I})$ for $t = 1, \dots, 300$ where $\mathbf{I} \in R^{3 \times 3}$ is the identity matrix.

The results can be seen in Table 5. Starting from setting of $C = 2$, most algorithms are able to perform well. DC-DS, CECPD and VPWBS achieve high F1-scores above 0.95, showing their effectiveness in the baseline setting. DC-DS is able to achieve the highest adjusted Rand of 0.991, showing that the partition it finds is the most accurate to the true partition. DC-DS is the most precise at finding the exact changepoint locations. For the setting of $C = 1$ and $C = 0.5$, DC-DS once again achieves the best Rand average and adjusted Rand average. DC-DS, CECPD, VPWBS all achieve similar level of F1-scores. In the precision-recall trade-off for the setting $C = 0.5$, DC-DS achieves best recall of 0.55 while CECPD achieves the best precision of 0.92. This supports findings in Section 3.1 for change in mean. Overall, this illustrates DC-DS is competitive, albeit a bit better, than other changepoint algorithms in the baseline setting.

Table 5: Change in Regression with Multiple Predictors

Mag. of Change	Algorithms	Rand Avg.	Adj. Rand Avg.	Precision	Recall	F1-score
2	DC-DS	0.991 _(0.001)	0.981 _(0.002)	0.99	0.99	0.99
	SGL	0.902 _(0.004)	0.776 _(0.010)	0.13	1.00	0.23
	CECPD	0.987 _(0.001)	0.971 _(0.001)	0.99	0.99	0.99
	VPWBS	0.971 _(0.004)	0.937 _(0.008)	0.92	0.98	0.95
1	DC-DS	0.973 _(0.002)	0.935 _(0.005)	0.85	0.85	0.85
	SGL	0.886 _(0.004)	0.736 _(0.011)	0.13	1.00	0.23
	CECPD	0.826 _(0.027)	0.713 _(0.042)	0.97	0.73	0.83
	VPWBS	0.955 _(0.005)	0.902 _(0.011)	0.81	0.88	0.84
0.5	DC-DS	0.898 _(0.008)	0.782 _(0.016)	0.38	0.55	0.45
	SGL	0.678 _(0.015)	0.406 _(0.023)	0.14	0.40	0.21
	CECPD	0.558 _(0.027)	0.285 _(0.042)	0.92	0.28	0.42
	VPWBS	0.782 _(0.019)	0.575 _(0.028)	0.40	0.48	0.43

Table details results of the decoupled approach, SGL, CECPD and VPWBS on simulated data with standard Gaussian noise and three predictors with two changepoints at location 75 and 225. Three settings for magnitude of change (C) are simulated in this experiment.

Comparing DC-DS with its closest competitor SGL, we see two major issues with SGL for flagging changepoints. First, as SGL identifies changepoints using a penalized loss function with ℓ_1 penalty based on the data, it has a tendency to over-predict the number of changepoints. Without a normalizer ($\{\psi_{g,t}\}$), SGL tends to prefer predicting multiple small changes rather than one significant change, leading to high precision, very low recall and low F1-score. Second, cross-validation struggles to identify the correct tuning parameter for the loss. As seen in the results, the tuning parameter value selected lead to significant over-prediction. Due to its poor performance in the baseline setting, we will drop SGL from the rest of the simulations.

3.2.2 Change in Regression with Stochastic Volatility

For the next set of simulations, we examine how the performance of these changepoint algorithms deteriorate in the presence of heterogeneity. For the most part, we use the same setting as Section 3.2.1. 100 series of length 300 with two changepoints at location 75 and 225 will be generated. However, instead of Gaussian noise, the noise will follow stochastic volatility of order 1 seen in Equation 11. We set μ_ϵ to be 0, ϕ_ϵ to be 0.9, and $\sigma_{\epsilon,t}^2$ to be 1, simulating high auto-correlation which lead to regions of high/low volatility.

The results are shown in Table 6. In comparison to the results in Table 5, we see that the performances of all 3 algorithms decreased in this setting. This is to be expected as switching from

Table 6: Change in Regression with Stochastic Volatility

Mag. of Change	Algorithms	Rand Avg.	Adj. Rand Avg.	Precision	Recall	F1-score
2	DC-DS	0.960 _(0.007)	0.922 _(0.014)	0.89	0.86	0.88
	CECPD	0.883 _(0.015)	0.724 _(0.013)	0.63	0.89	0.73
	VPWBS	0.881 _(0.014)	0.752 _(0.025)	0.54	0.65	0.59
1	DC-DS	0.898 _(0.017)	0.814 _(0.028)	0.75	0.70	0.72
	CECPD	0.869 _(0.016)	0.700 _(0.015)	0.52	0.60	0.56
	VPWBS	0.758 _(0.019)	0.545 _(0.030)	0.39	0.35	0.37
0.5	DC-DS	0.777 _(0.019)	0.587 _(0.031)	0.42	0.43	0.42
	CECPD	0.726 _(0.019)	0.480 _(0.028)	0.20	0.18	0.19
	VPWBS	0.512 _(0.019)	0.185 _(0.025)	0.17	0.05	0.08

Table details results of DC-DS, CECPD and VPWBS on simulated data with stochastic volatility and three predictors with two changepoints at location 75 and 225. Three settings for magnitude of change (C) are simulated in this experiment.

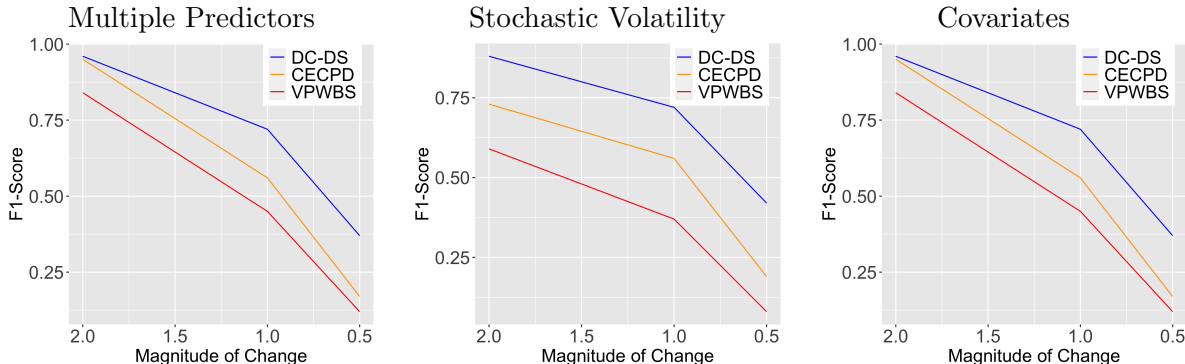
Gaussian noise to stochastic volatility makes changepoint identification much more difficult. DC-DS performs the best in terms of F1-score and average adjusted Rand in all three magnitude of change settings. DC-DS achieves a F1-score of 0.88 in magnitude of change 2 setting and 0.72 in magnitude of change 1 setting. CECPD comes in second place with a F1-score of 0.73 in magnitude of change 2 setting and 0.56 in magnitude of change 1 setting. VPWBS struggles more in this setting as the algorithm is not intended to work in presence of heterogeneity.

In presence of stochastic volatility, the gap between DC-DS widened in terms of both F1-score and adjusted Rand. average. This shows that DC-DS is more precise at finding the correct changepoint locations. The results illustrate further support for one of the major advantages of the decoupled approach: the robustness and flexibility of Bayesian DLM in dealing with heterogeneity make the decoupled approach more adaptive to complex datasets.

3.2.3 Change in Regression with Covariates

For the final set of simulations, we evaluate the performance of the decoupled approach against other changepoint algorithms when covariates are added to the model. We simulate 100 series of length 300 with one changepoint at location 150. For each series, we generate one predictor series $\{x_t\}_{t=1}^{300}$ and two covariate series $\{z_{t,1}\}_{t=1}^{300}$, $\{z_{t,2}\}_{t=1}^{300}$. The relationship between the response, the

Figure 4: Change in Regression: Comparison of F1-Scores



The left plot shows F1-score of DC-DS (blue line) against CECPD (orange line) and VPWBS (red line) in simulated regression with multiple predictors and Gaussian noise from Section 3.2.1. The middle plot shows F1-score comparisons in simulated regression with stochastic volatility from Section 3.2.2. The right plot shows F1-score comparisons in simulated regression with covariates from Section 3.2.3.

predictor and the covariates are as follows:

$$y_t = \begin{cases} \beta_1 x_t + \alpha_1 z_{t,1} + \alpha_2 z_{t,2} + \epsilon_t & t \leq 149 \\ \beta_2 x_t + \alpha_1 z_{t,1} + \alpha_2 z_{t,2} + \epsilon_t & t \geq 150 \end{cases}$$

where $\{\epsilon_t\}$ is a standard Gaussian noise, $(\beta_1, \beta_2) = (0, C)$, and $(\alpha_1, \alpha_2) = (0.3, 0.1)$. The predictor series is generated from $x_t \sim_{i.i.d.} N(0, 1)$ and the covariate series are generated from $z_{t,1}, z_{t,2} \sim_{i.i.d.} \text{Bern}(0.5)$ where $\text{Bern}(\cdot)$ are samples from the Bernoulli distribution. As seen, the covariates relationship with y does not change over-time while one changepoint exist for the predictor series.

Table 7 details the results for this set of simulations. As seen, DC-DS outperforms the competing methods and the advantage becomes more significant as the signal-to-noise ratio decreases. In the highest setting for magnitude of change of 2, DC-DS, CECPD and VPWBS all perform well in terms of adjusted Rand average and F1-score. This is due to the fact that the change in predictor is significantly greater than the impact of the covariates. However, as the magnitude of change decreases to 1, we can see competing methods' performances begin to deteriorate. This is to be expected as CECPD and VPWBS have no way to distinguish the covariates from the predictor. DC-DS, on the other hand, maintains a high F1-score of 0.72 and adjusted Rand average of 0.899 in this setting. With a Bayesian DLM separating the impact of covariates from predictor, DC-DS is able to produce correct coefficient estimates. This advantage becomes more apparent as magnitude

Table 7: Change in Regression with Covariates

Mag. of Change	Algorithms	Rand Avg.	Adj. Rand Avg.	Precision	Recall	F1-score
2	DC-DS	0.987 _(0.002)	0.974 _(0.004)	0.96	0.96	0.96
	CECPD	0.981 _(0.002)	0.961 _(0.003)	0.95	0.95	0.95
	VPWBS	0.961 _(0.005)	0.922 _(0.010)	0.78	0.90	0.84
1	DC-DS	0.949 _(0.007)	0.899 _(0.014)	0.72	0.73	0.72
	CECPD	0.908 _(0.009)	0.816 _(0.018)	0.48	0.72	0.56
	VPWBS	0.850 _(0.014)	0.701 _(0.028)	0.38	0.55	0.45
0.5	DC-DS	0.767 _(0.021)	0.535 _(0.041)	0.44	0.31	0.37
	CECPD	0.565 _(0.016)	0.133 _(0.033)	0.67	0.10	0.17
	VPWBS	0.681 _(0.020)	0.365 _(0.040)	0.15	0.10	0.12

Table details results of the decoupled approach, CECPD and VPWBS on simulated data with standard Gaussian noise, one predictor with one changepoint at location $\{150\}$ and 2 covariates. Three settings for magnitude of change (C) are simulated in this experiment.

of change decreases to 0.5. In this setting, the predictor series and the covariates have a similar impact on the response. As a result, no other changepoint algorithm can reliably identify the correct changepoint location (the highest competing F1-score being CECPD at 0.17). DC-DS, in this setting, achieves a F1-score of 0.37, showing its robustness.

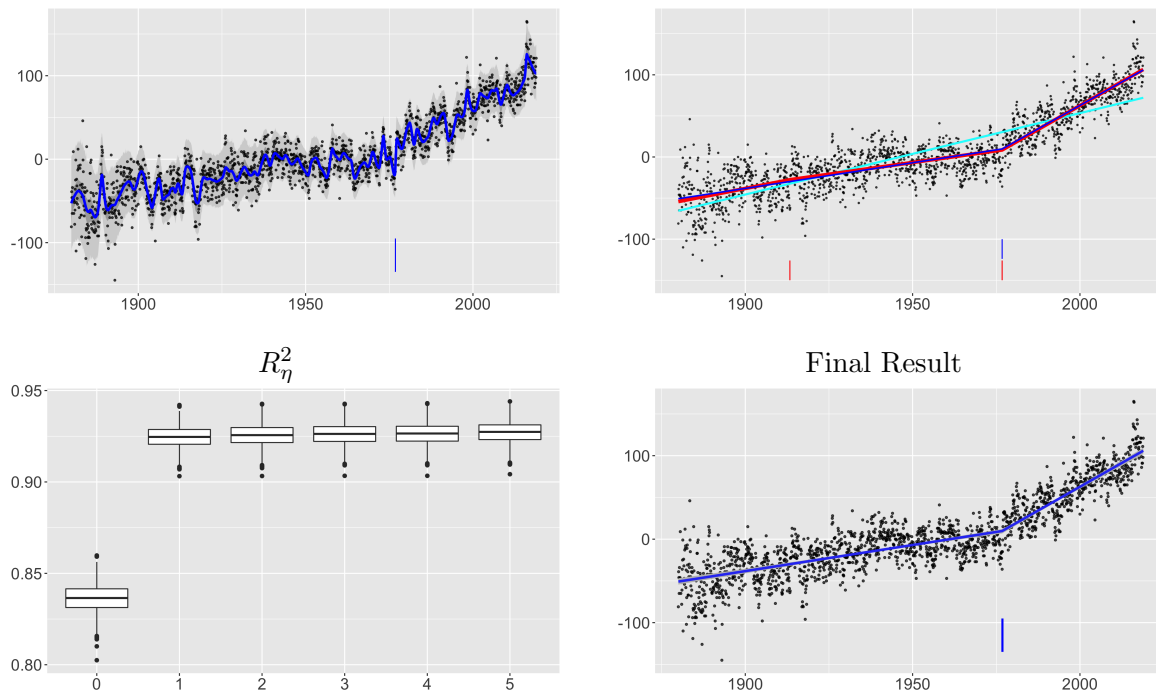
Figure 4 summarizes the F1-score results of DC-DS against the competing methods for all 3 regression simulation settings. As seen in the plot, all three algorithms perform similarly well in the baseline setting with Gaussian noise. However, as the scenarios become more complicated such as when stochastic volatility is added or covariates are included, the advantages of DC-DS become more apparent. This further highlights the advantage of the decoupled approach in its ability to fit a highly complex Bayesian DLM to the underlying data to deal with complications inherent in series.

4 Real World Examples

4.1 Global Land Surface Air Temperature Example

For an illustrative application we consider monthly global land surface air temperature from 1880 to 2018. The data is made available on National Aeronautics and Space Administration website (https://data.giss.nasa.gov/gistemp/tabledata_v3/GLB.Ts.txt) and has been previously analyzed (Yang and Song, 2014). Identifying changes in climate patterns has become an urgent area of analysis (Alley *et al.*, 2003). Understanding when the underlying dynamics of global

Figure 5: Monthly Global Land Surface Air Temperature
Bayesian DLM Results Projected Posteriors



The top-left figure shows the monthly average global land surface air temperature from 1880 to 2018. Blue line shows predicted mean from Bayesian DLM with 95% credible bands for $\{\beta_t\}$ in dark gray and 95% credible bands for $\{\beta_t + \epsilon_t\}$ in light gray. Change point predicted by the decoupled approach is shown by blue vertical line. The top-right figure shows the mean of “projected posterior” for $\{0, 1, 2\}$ change points (in cyan, blue and red respectively). The predicted change point locations are shown by the same colored vertical lines. The bottom left plot illustrates the distribution R_η^2 for various number of change points. The bottom right plot shows the final result for the decoupled approach.

temperature pattern shifts can be very important in policy decision making. The top panel in Figure 5 shows the recorded global land surface air temperature. As shown, there are clear long term linear time trends underlying local annual trends in the data. Overall global temperature appear increasing over time; however, three features make standard changepoint analysis difficult. First, there exists seasonal fluctuation in the data, and these seem somewhat irregular. This implies the local trend is not flat but rather a smooth curve fluctuating through the months. Second, there is differing levels of variability over time. Third, there may be anomalies throughout the data as a result of certain global events.

As seen in the top-left plot of Figure 5, the underlying signal fluctuates over time as a result of irregular cyclical patterns over the years; these patterns have less variability than the longer term

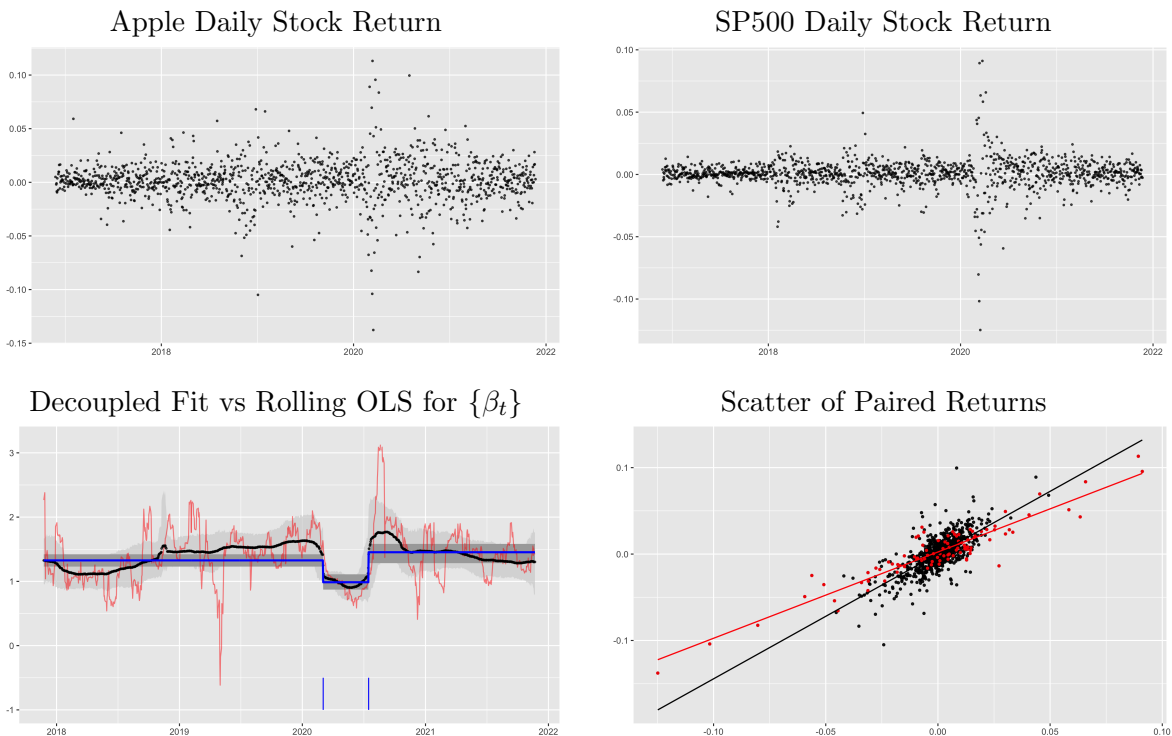
approximately linear time trends. This results in a very wiggly fit from the Bayesian dynamic linear model with $D = 2$. Using the decoupled approach, we can visualize different fits of the projected posterior. The top-right plot of Figure 5 illustrates the mean of the “projected posterior” for $\{0, 1, 2\}$ number of changepoints. As seen in the figure, as the number of changepoints increase, the fit becomes increasingly better. This is because increasing the number of changepoints essentially increases the degrees of freedom for the “projected posterior”. We select 1 as the optimal number of changepoints as it’s the simplest fit in which the upper 90% credible interval exceeds the 0.9 threshold. We see from bottom plot of Figure 5 that additional changepoints do not significantly increase R_η^2 and seem to overfit the data. We find the single changepoint around the year 1963, after which there is a steeper long term slope.

4.2 Financial Data

For the next application, we apply the decoupled approach, with $D = 1$, for identifying changepoint in financial stock returns. The data is publicly available through Yahoo Finance. Stock returns represent a significant challenge for changepoint analysis due to its low signal-to-noise ratio. Many methods have been previously utilized for identifying changepoint in this area such as regime switching model (Hardy, 2001), penalized likelihood via dynamic programming (Bai and Perron, 2002), and Bayesian optimal stopping time model (Shiryaev *et al.*, 2014). We choose to focus on Apple stocks as it’s one of the largest companies in the market place and represent a significant portion of the market indices. Apple stock returns have been analyzed for changepoints in previous works (van den Burg and Williams, 2020; Lleo *et al.*, 2020). Lleo *et al.* (2020) applied many changepoint algorithms for an in-depth analysis for apple stock return; they primarily found breaks in variance. In this application, we will focus on the regression setting, analyzing changes in relationship between Apple and the market across the last 5 years. Building of foundations of Capital Asset Pricing Model (Sharpe, 1964), identifying changes in the coefficient between a particular asset and the market can provide key information for portfolio optimization. Note that while we chose Apple return for this example, the same analysis can be performed for any other assets.

We collected daily closing price of Apple stock and S&P 500 over the last 4 years and calculate daily log return for both assets. We regressed daily Apple return on S&P 500 return to calculate the beta for the stock. Figure 6 illustrate the results. As seen, the return data for Apple and S&P 500 are quite noisy and exhibit regions of high and low volatility. This makes changepoint

Figure 6: Apple Asset Return Plots



The top-left plot shows the distribution of daily return over the past 4 years for Apple. The top-right plot shows the distribution of daily return over the past 4 years for S&P 500. The bottom-left plot shows the Bayesian DLM estimate (black) in comparison with a 22 day rolling ordinary least squares (red) for coefficient beta. The estimated credible bands for Bayesian DLM in shown in dark gray. As seen, the Bayesian DLM produces much a smoother estimate for $\{\beta_t\}$. In addition, the resulting decoupled fit in shown blue line with two changepoints in blue vertical bars. The 95% credible bands for “projected posterior” is shown in dark gray and the 95% credible bands from Bayesian DLM is shown in light gray. The bottom right plot shows a scatter plot of apple return vs S&P 500 return. The points are color coded by the decoupled approach’s selected changepoints. Returns before the first changepoint (03/02/2020) and after the second changepoint (07/22/20) are colored in black; returns between the first changepoint and the second changepoint are colored in red. The lines represent correlation line of best fit for the color coded points.

detection quite difficult. Competing methods such as CECPD and VPWBS identify no changepoints in this regression context. However, the decoupled approach identifies two changepoints at location 03/02/2020 and 07/22/2020. These dates mark the beginning of the pandemic where significant volatility occurred within the stock market. These changepoints can be supported through a simple correlation analysis. The correlation of daily return between Apple and S&P 500 before 03/02/2020 is around 0.73; correlation from 03/02/2020 to 07/22/2020 is around 0.93 and corre-

lation after 07/22/2020 is around 0.69. As seen, the returns become significantly more correlated during this time period. Unlike other time periods where changes in beta is gradual, we see drastic change in beta as a result of the pandemic which induces the estimation of changepoints. The decoupled approach is the only method to estimate changepoints in this period, further illustrating its robustness.

5 Conclusion

In conclusion, the paper proposes a decoupled approach for changepoint analysis that separates the processing of modeling and inference. First, a Bayesian dynamic linear model is fit to the underlying data to estimate the relationship between the predictor series and the response series. Bayesian DLM is a popular tool for time series analysis and can deal with many complexities inherent in the data such as outliers and heterogeneity. With incorporation of shrinkage priors, Bayesian DLM can fit a complex model to the underlying data while producing smooth estimates of the underlying coefficients. Second, utilizing the posterior draws of a Bayesian DLM, we derive a decoupled weighted least square loss to estimate the number of changepoints. The loss is composed of a goodness-of-fit term for posterior mean of the Bayesian DLM and a penalty term for the number of changepoints. The weights for each time-step is chosen to be the inverse of the estimated variance; making the approach more robust regions of high/low volatility.

As seen throughout the simulations and real world examples, the decoupled approach offers two key advantages over the competing method. First, by separating the process of modeling and inference, the decoupled approach allows for fitting of a highly complex Bayesian model to the underlying data while still allowing for reasonable inference of changepoints. This allows the decoupled approach to deal with many complexities inherent in time series. As the data becomes increasing complex, the decoupled approach can adapt the Bayesian DLM to deal with these issues while maintaining the same inference process for changepoints. Second, the decoupled approach is flexible in its ability to identify different types of changepoints. From the examples, we have shown that the decoupled approach's ability to identify changes in mean, changes in regression coefficients and changes in higher order trends. In addition, the decoupled approach can effectively identify changepoints in presence of covariates. Most other changepoint algorithms can only be utilized for one specific scenario. The flexibility of the decoupled approach allow the algorithm to be more adaptive to a wide variety of datasets.

References

- Adams, R. P., and MacKay, D. J. (2007). “Bayesian online changepoint detection,” arXiv:0710.3742 .
- Alley, R. B., Marotzke, J., Nordhaus, W. D., Overpeck, J. T., Peteet, D. M., Pielke, R., and et al. (2003). “Abrupt climate change,” *Science* **299**, 2005–2010.
- Aminikhanghahi, S., and Cook, D. J. (2017). “A survey of methods for time series change point detection,” *Knowledge Information System* **51**, 339–367.
- Bai, J., and Perron, P. (2002). “Computation and analysis of multiple structural change models,” *Journal of Applied Econometrics* **18**, 1–22.
- Banbura, M., Giannone, D., and Reichlin, L. (2010). “Large bayesian vector auto regressions,” *Journal of Applied Econometrics* **25**, 71–92.
- Bashir, A., Carvalho, C. M., Hahn, P. R., and Jones, M. B. (2019). “Post-processing posteriors over precision matrices to produce sparse graph estimates.,” *Bayesian Analysis* **14**, 1075–1090.
- Belmonte, M. A., Koop, G., and Korobilis, D. (2013). “Hierarchical shrinkage in time-varying parameter models,” *Journal of Forecasting* **33**, 80–94.
- Bhadra, A., Datta, J., Polson, N. G., and Willard, B. (2016). “Default bayesian analysis with global-local shrinkage priors,” *Biometrika* **103**, 955–969.
- Bitto, A., and Fruhwirth-Schnatter, S. (2019). “Achieving shrinkage in a time-varying parameter model framework,” *Journal of Econometrics* **210**, 75–97.
- Carvalho, C. M., Polson, N. G., and Scott, J. G. (2009). “Handling sparsity via the horseshoe,” *AISTATS* **5**, 73–80.
- Chan, J. C. C., and Eisenstat, E. (2018). “Bayesian model comparison for time-varying parameter vars with stochastic volatility,” *Journal of Applied Econometrics* **33**, 509–532.
- Ciuperca, G. (2014). “Model selection by lasso methods in a change-point model,” *Stat. Papers* **55**, 349–374.
- Ciuperca, G., and Maciak, M. (2019). “Change-point detection in a linear model by adaptive fused quantile method,” *Scandinavian Journal of Statistics* **47**, 425–463.

- Eckley, I. A., Fearnhead, P., and Killick, R. (2011). “Analysis of changepoint models,” *Bayesian time series models* 205–224.
- Erdman, C., and Emerson, J. W. (2008). “A fast bayesian change point analysis for the segmentation of microarray data,” *Bioinformatics* **24**, 2143–2148.
- Fearnhead, P. (2006). “Exact and efficient bayesian inference for multiple changepoint problems,” *Statistics and computing* **16**(2), 203–213.
- Fearnhead, P., and Liu, Z. (2011). “Efficient bayesian analysis of multiple changepoint models with dependence across segments,” *Statistics and Computing* **21**(2), 217–229.
- Fearnhead, P., and Rigaiil, G. (2019). “Changepoint detection in the presence of outliers,” *Journal of the American Statistical Association* **114**, 169–183.
- Friedman, J., Hastie, T., and Tibshirani, R. (2010). “Regularization paths for generalized linear models via coordinate descent,” *Journal of Statistical Software* **33**(1), 1–22.
- Fryzlewicz, P. (2014). “Wild binary segmentation for multiple change-point detection,” *Annals of Statistics* **42**, 2243–2281.
- Green, P. J. (1995). “Reversible jump markov chain monte carlo computation and bayesian model determination,” *Biometrika* **82**(4), 711–732.
- Green, P. J. (2003). “Trans-dimensional markov chain monte carlo,” *Oxford Statistical Science Series* 179–198.
- Guidolin, M., Hansen, E., and Pedio, M. (2019). “Cross-asset contagion in the financial crisis: A bayesian time-varying parameter approach,” *Journal of Financial Markets* **45**, 83–114.
- Hahn, P. R., and Carvalho, C. M. (2015). “Decoupling shrinkage and selection in bayesian linear models: A posterior summary perspective,” *Journal of American Statistical Association* **110**, 435–448.
- Harchaoui, Z., Moulines, E., and Bach, F. (2008). “Kernel change-point analysis,” *Advances in Neural Information Processing Systems* **27**, 519–533.
- Hardy, M. R. (2001). “A regime-switching model of long-term stock,” *North American Actuarial Journal* **5**, 41–53.

- James, N. A., and Matteson, D. S. (2014). “ecp: An r package for nonparametric multiple change point analysis of multivariate data,” *Journal of Statistical Software* **62**, 1–25.
- Jeske, D. R., Montes De Oca, V., Bischoff, W., and Marvasti, M. (2009). “Cusum techniques for timeslot sequences with applications to network surveillance,” *Computational Statistics and Data Analysis* **53**, 4332–4344.
- Jin, B., Wu, Y., and Shi, X. (2016). “Consistent two-stage multiple change-point detection in linear models,” *Canadian Journal of Statistics* **44**, 161–179.
- Kiers, H. A. L. (1997). “Weighted least squares fitting using ordinary least squares algorithm,” *Psychometrika* **62**, 251–266.
- Killick, R., Fearnhead, P., and Eckley, A. (2012). “Optimal detection of changepoints with a linear computational cost,” *Journal of American Statistical Association* **107**, 1590–1598.
- Kim, S., Shephard, N., and Chib, S. (1998). “Stochastic volatility: Likelihood inference and comparison with arch models,” *Review of Economic Studies* **65**, 361–393.
- Ko, S. I., Chong, T. T., and Ghosh, P. (2015). “Dirichlet process hidden markov multiple change-point model,” *Bayesian Analysis* **10**(2), 275–296.
- Kowal, D., Matteson, D., and Ruppert, D. (2019). “Dynamic shrinkage process,” *J. R. Statist. Soc. B* **81**.
- Kowal, D. R., and Bourgeois, D. C. (2020). “Bayesian function-on-scalars regression for high dimensional data,” .
- Leonardi, F., and Bühlmann, P. (2016). “Computationally efficient change point detection for high-dimensional regression,” *arXiv:1601.03704* .
- Liu, S., Yamada, M., Collier, N., and Sugiyama, M. (2013). “Change-point detection in time-series data by relative density-ratio estimation,” *Neural Networks* **43**, 72–83.
- Lleo, S., Ziemba, W. T., and Li, J. (2020). “Exploring breaks in the distribution of stock returns: Empirical evidence from apple inc.,” Available at SSRN: <https://ssrn.com/abstract=3700419> .
- Maidstone, R., Hocking, T., Rigaiil, G., and Fearnhead, P. (2017). “On optimal multiple change-point algorithms for large data,” *Statistics and Computings* **27**, 519–533.

- Matteson, D. S., and James, N. A. (2014). “A nonparametric approach for multiple change point analysis of multivariate data,” *Journal of the American Statistical Association* **109**, 334–345.
- Nakajima, J., Kasuya, M., and Watanabe, T. (2011). “Bayesian analysis of time-varying parameter vector autoregressive model for the Japanese economy and monetary policy,” *Journal of The Japanese and International Economies* **25**, 225–245.
- Park, T., and Casella, G. (2008). “The bayesian lasso,” *Journal of the American Statistical Association* **103**, 681–686.
- Pichuka, S., and Maity, R. (2018). “Development of a time-varying downscaling model considering non-stationarity using a bayesian approach,” *International Journal of Climatology* **38**, 3157–3176.
- Puelz, D., Carvalho, C. M., and Hahn, P. R. (2015). “Optimal etf selection for passive investing,” .
- Qian, J., and Su, L. (2016). “Shrinkage estimation of regression models with multiple structural changes,” *Econometric Theory* **32**, 1376–1433.
- Sharpe, W. F. (1964). “Capital asset prices: A theory of market equilibrium under conditions of risk,” *The journal of finance* **19**(3), 425–442.
- Shiryaev, A. N., Zhitlukhin, M. V., and Ziemba, W. T. (2014). “Land and stock bubbles, crashes and exit strategies in Japan circa 1990 and in 2013,” *Quantitative Finance* **15**, 1449–1469.
- Siems, T., Hellmuth, M., and Liebscher, V. (2019). “Simultaneous credible regions for multiple changepoint locations,” *Journal of Computational and Graphical Statistics* **28**(2), 290–298.
- van den Burg, G. J. J., and Williams, C. K. I. (2020). “An evaluation of change point detection algorithms,” .
- Wang, D., Zhao, Z., Lin, K. Z., and Willett, R. (2021). “Statistically and computationally efficient change point localization in regression settings,” *Journal of Machine Learning Research* **22**, 1–46.
- Woody, S., Carvalho, C. M., and Murray, J. S. (2020). “Model interpretation through lower-dimensional posterior summarization,” .
- Wu, H., and Matteson, D. S. (2020). “Adaptive bayesian changepoint analysis and local outlier scoring,” *arXiv preprint arXiv:2011.09437* .

- Yang, Y., and Song, Q. (2014). “Jump detection in time series nonparametric regression models: a polynomial spline approach,” *Annals of the Institute of Statistical Mathematics* **66**, 325–344.
- Yuan, M., and Lin, Y. (2007). “Model selection and estimation in regression with grouped variables,” *Journal of the Royal Statistical Society, Series B* **68**, 49–67.
- Zhang, B., Geng, J., and Lai, L. (2015). “Multiple change-points estimation in linear regression models via sparse group lasso,” *IEEE Transactions on Signal Processing* **63**.
- Zhang, W., Gilbert, D., and Matteson, D. S. (2019). “Abacus: unsupervised multivariate change detection via bayesian source separation,” in *Proceedings of the 2019 SIAM International Conference on Data Mining*, SIAM, pp. 603–611.
- Zou, H. (2006). “The adaptive lasso and its oracle properties,” *Journal of the American Statistical Association* **101**, 1418–1429.